J|A|C|S COMMUNICATIONS

Published on Web 06/03/2010

Characterization of RNA Invasion by ^{19}F NMR Spectroscopy

Anu Kiviniemi and Pasi Virta*

Department of Chemistry, University of Turku, FIN-20014 Turku, Finland

Received February 22, 2010; E-mail: pasi.virta@utu.fi

Invasion is a fundamental process of RNA, in which a weak stem region is denatured by an exterior single strand (*i.e.*, "invader"), resulting in a reorganized secondary structure. This process, applied, *e.g.*, in the antisense approach,[1] is well known, but the means with which to follow its progress in detail are rather limited. For example, the invasion cannot be clearly detected by a thermal UV-denaturation profile or by fluorescence or CD spectra, since what happens is conversion of a double helix to another double helix. Gel shift assay in principle allows determination of the equilibrium constants for this kind of a chain invasion, but it may skew the equilibrium between weakly interacting species. NMR spectroscopy is devoid of such limitations and offers an efficient tool for the analysis of such dynamic equilibria.[2] ^{1}H NMR spectroscopic detection of the imino protons is a feasible option, but the reliance on the integrity of Watson−Crick base pairs may be a limitation at elevated temperatures. Additionally, the small chemical dispersion of ^{1}H detection may lead to a signal overlap. Although this problem could partly be overcome by more time-consuming 2D methods,[3] a technique based on labeling with a biologically nonexistent nucleus appears more attractive. Recently, the potential of ^{19}F NMR spectroscopy as a tool for analysis of RNA secondary structures has been recognized.[4] ^{19}F is a sensitive nucleus (83% compared to ^{1}H), and its resonance shift is additionally strongly dependent on the spatial vicinity of the ^{19}F label.[5] Thus, even a modest change in the secondary structure of a ^{19}F-labeled RNA may result in a detectable resonance signal distinct from that of the initial state. Recently, 2′-deoxy-2′-fluoronucleosides incorporated in RNA have been used for the identification of site-specific RNA binders:[4d] 5-[4,4,4,-trifluoro-3,3-bis(trifluoromethyl)but-1-ynyl]-2′-deoxyuridine for the detection of DNA duplex formation,[4f] 5-fluoropyrimidine nucleotides for the characterization of secondary structure of HIV-2 TAR[6] (Trans Activation Response Element) RNA,[4e] and 2′-deoxy-2′-fluoro- and 2,4-difluorotoluene nucleosides for the quantification of hairpin/hairpin[4a] and duplex/hairpin[4g] equilibria of self-complementary RNAs. The latter[4g] is an excellent example how a temperature-dependent shift of ^{19}F resonances can be used for the analysis of dynamic equilibria of secondary structures. RNA invasion represents a related but even a more complex reaction system. The present study offers the first example of the applicability of ^{19}F NMR spectroscopy to elucidation of the course of such a process. Invasion of 2′-*O*-methyl oligoribonucleotides into a ^{19}F-labeled HIV-1 TAR RNA model and the temperature-dependent behavior of the complexes obtained have been examined. Additionally, the influence of a known TAR ligand, *viz.* neomycin B,[7] on the invasion has been demonstrated.

Among the potential fluorine-labeled probes, recently described 5-[4,4,4-trifluoro-3,3-bis(trifluoromethyl)but-1-ynyl]-2′-deoxyuridine[4f] was adopted for the experiments. It bears nine magnetically equivalent fluorine atoms, which allows rapid measurements at a micromolar RNA concentration. Additionally, the fluorine atoms of this probe are not magnetically coupled to protons, which provides resonance signals as singlets without fluorine−proton decoupling.[4a,8] The fluorinated nucleoside was incorporated into the TAR model in place of the uridine nucleoside within the tetranucleotide stem between the loop and the bulge of the native TAR structure (**A** in Scheme 1). A ^{19}F resonance signal distinct from that referring to the initial hairpin structure (**A**) may hence be expected when a structural change, such as invasion (**C** or **D**) or thermal denaturation (**B**), takes place. Two 2′-*O*-methyl ribonucleotides were inserted to both the 5′- and 3′-ends to increase the stability of the 3′/5′-stem region and to protect the model against degradation by exonucleases.

Scheme 1

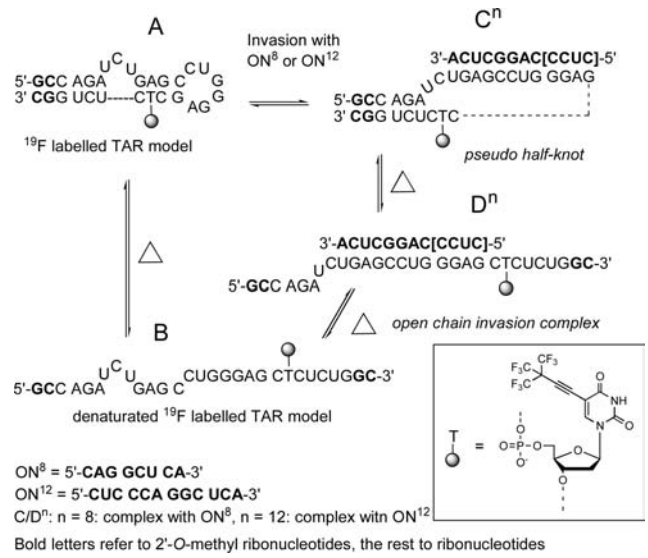

First the applicability of an appropriately positioned ^{19}F probe to determination of the melting temperature of our TAR model (see **A**→**B** in Scheme 1) was evaluated. At 25 °C, the probe gives one sharp ^{19}F resonance signal at −66.32 ppm, which upon heating expectedly undergoes a linear temperature-dependent shift downfield (traces i−iv in Figure 1, slope 0.014 ppm K^{-1}; note the reference signal with the same value). On approaching the T_m value (v−vii in Figure 1), this signal is broadened and a new broad signal appears 0.4 ppm upfield. The latter signal most likely refers to the denaturated form **B** of the TAR model. In other words, the equilibration between the double-helical (**A**) and single-stranded (**B**) forms of the TAR model is slow on the NMR time scale below the melting temperature. Upon further heating, the signals shift closer to each other, being almost equal sized at 60 °C (∼T_m, vii in Figure 1). Coalescence to the broad signal at −66.32 ppm is observed at 66 °C (vi in Figure 1). According to the shift, this signal refers to a mixture in which **B** predominates. After completion of the denaturation process (>70 °C), the signal is sharpened and a linear temperature-dependent shift downfield (vii in Figure 1) is again observed. As seen in Figure 2a(ii), a unique negative *S*-curve (^{19}F shift *vs* temperature) is obtained. The sharp inflection point of

10.1021/ja1014629

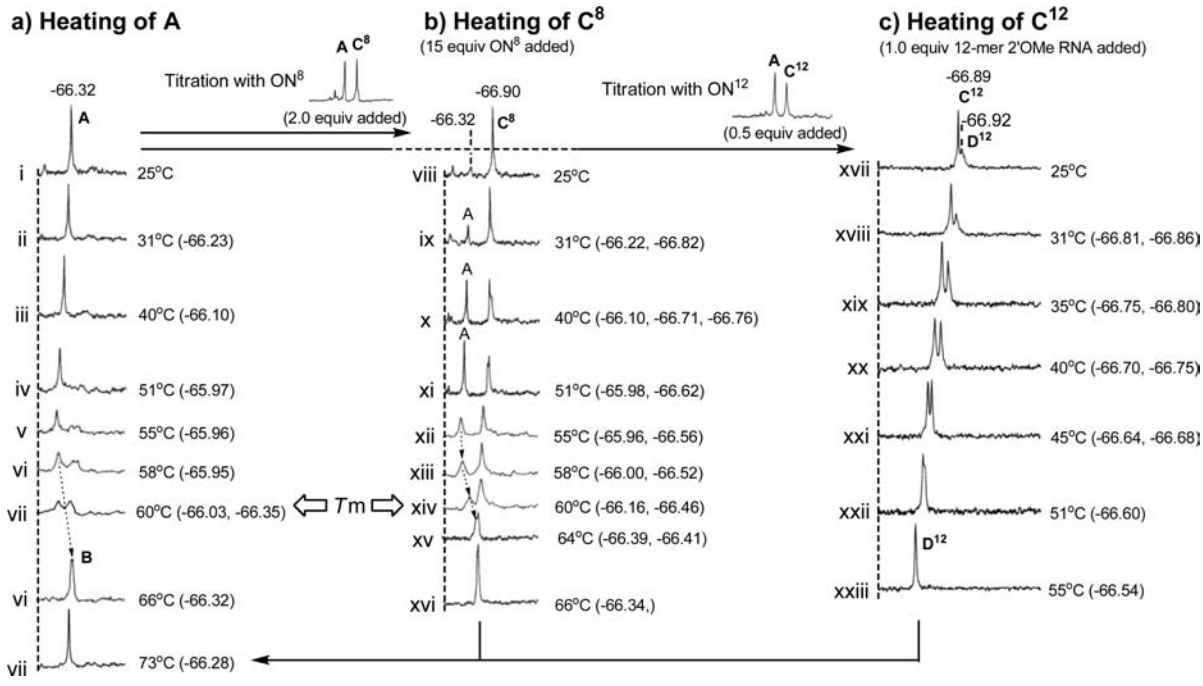

Figure 1. ^{19}F NMR spectra of the ^{19}F-labeled TAR model **A** (a) and its invasion complexes **C**^{8}→**D**^{8} (b) and **C**^{12}→**D**^{12} (c) at different temperatures.

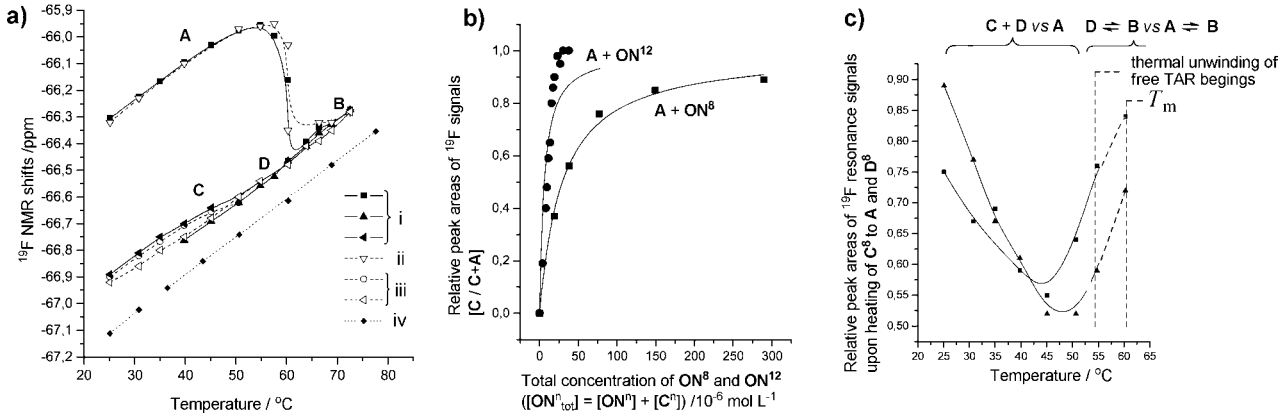

Figure 2. (a) Profiles of the ^{19}F NMR resonance shifts *versus* temperature. Shifts obtained by heating (i) **C**^{8}, (ii) **A**, (iii) **C**^{12} (cf. Scheme 1 and Figure 1), and (iv) 5-[4,4,4-trifluoro-3,3-bis(trifluoromethyl)but-1-ynyl]-2′-deoxyuridine as a reference. Conditions: (i) 20 μmol L^{-1} **A** and 290 μmol L^{-1} **ON**^{8} in 25 mmol L^{-1} NaH_2PO_4-buffered H_2O-D_2O (5:1 v/v, pH 6.5); (ii) 20 μmol L^{-1} **A** in the same buffer; (iii) 20 μmol L^{-1} **A** and 20 μmol L^{-1} **ON**^{12} in the same buffer. (b) Titration of **A** with **ON**^{8} and **ON**^{12}. (**C**/**C** + **A**) obtained by integrals of ^{19}F resonances at different concentrations of 2′-*O*-methyl oligoribonucleotide. ●, 5′-CUC CCA GGC UCA-3′ (K_d = 5.6 ± 1.2 μmol L^{-1}); ■, 5′-CAG GCU CA-3′ (K_d = 28.9 ± 1.5 μmol L^{-1}). Conditions: 20 μmol L^{-1} **A** + increasing concentration of **ON**^{8} or **ON**^{8} in the same buffer at 25 °C. (c) Relative peak areas of the ^{19}F resonance signals upon heating of the invasion complex **C**^{8} (to **A** and **D**^{8}) in the presence (■) and absence (▲) of neomycin. Conditions: ▲, cf. panel a (i); ■, 20 μmol L^{-1} **A**, 40 μmol L^{-1} **ON**^{8}, and 20 μmol L^{-1} neomycin in the same buffer.

the curve refers to thermal denaturation, consistent with the profile obtained by UV spectroscopy (T_m = 60.7 °C).

HIV-1 TAR element is a widely used target for the antisense oligonucleotides.[9] It occurs at the 5′-end of all HIV-1 RNA transcripts and is regulated by trans activator protein Tat during transcriptional elongation. Two 2′-*O*-methyl oligoribonucleotide invaders, *viz.* 5′-CUC CCA GGC UCA-3′ (**ON**^{12}) and 5′-CA GGC UCA-3′ (**ON**^{8}), were chosen as invaders for our TAR model. The 12-mer **ON**^{12} inhibits Tat-dependent *in vitro* transcription in HeLa cell nuclear extract.[9d] Additionally, a pseudo-half-knotted TAR RNA complex has been reported to be formed with the two-nucleotide-shifted 12-mer 5′-CCC AGG CUC ACA-3′.[9b] A weak interaction is expected to occur between **ON**^{8} and TAR model **A**. This kind of a dynamic equilibrium is of special interest, since it is difficult to study by other methods. It is worth noting that the fluorine label in our TAR model decreases the stability of the four-nucleotide stem between the bulge and the loop (T_m = 60.7 °C compared to 63.4 °C for the corresponding nonlabeled structure), which undoubtedly facilitates invasion. Upon titration of **A** with **ON**^{12} at 25 °C (see **A**→**C**^{12} and **D**^{12} in Scheme 1), the signal of **A** disappears, and a novel signal at −66.89 ppm (xviii in Figure 1) appears almost quantitatively (K_d = 5.6 ± 1.2 μmol L^{-1} at 25 °C, Figure 2b), referring most likely to formation of **C**^{12} by chain invasion. Interestingly, on increasing the temperature, gradual conversion of this signal to another one 0.05 ppm upfield takes place (xvii−xxii in Figure 1), the two signals being equal at 45 °C (xxi in Figure 1). At 51 °C, they are merged to a single broad signal (xxii in Figure 1). As mentioned above, a pseudo-half-knotted TAR RNA complex has previously been characterized.[9b] Most likely, the first observed signal refers to a macro-looped complex that resembles the half-knot (**C**^{12} in Scheme 1) and the latter signal to a stable open-chain invasion complex (**D**^{12} in Scheme 1). When the temperature is further increased, the signal of **D**^{12} is almost linearly shifted downfield, and eventually it merges

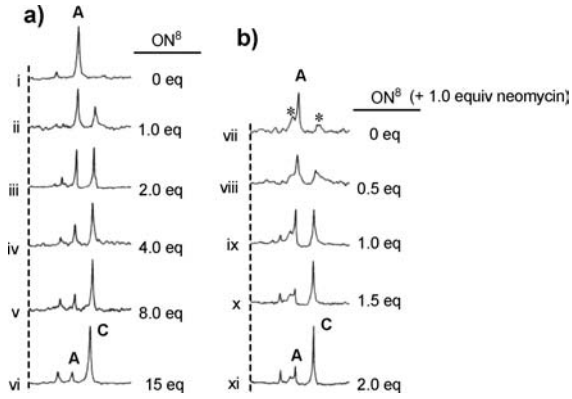

Figure 3. ^{19}F NMR spectra upon titration of **A** with **ON^8** in the absence (a, ii−vi) and in the presence (b, viii−xi) of neomycin. Conditions: (i−vi) 20 μmol L^{-1} **A** + increasing concentration of **ON^8** in 25 mmol L^{-1} NaH_2PO_4-buffered H_2O-D_2O (5:1 v/v, pH 6.5) at 25 °C; (vii−xi) cf. conditions i−vi + 20 μmol L^{-1} of neomycin.

with the signal of the single-stranded form **B** of the TAR model (iii in Figure 2a). Thermal denaturation of **D^{12}**, hence, takes place at a higher temperature than the conversion of the hairpin TAR (**A**) to an open-chain form (**B**), consistent with the T_m value of 65.7 °C obtained by thermal UV profile. The signals of **D^{12}** and **B** overlap as expected, since the melting of **D^{12}** is not accompanied by any marked change in the immediate vicinity of the ^{19}F probe. The temperature-dependent behavior of the **C^{12}→D^{12}** complex was additionally characterized by ^{1}H NMR spectroscopy of the imino region (see Supporting Information), which supported observed ^{19}F NMR data.

Titration with an 8-mer oligonucleotide, **ON^8**, could also be successfully monitored. As expected, the affinity is weak, but a 1:1 complex is formed ($K_d = 28.9 \pm 1.5$ μmol L^{-1} at 25 °C, Figure 2b). At 25 °C and in an excess (15 equiv) of **ON^8**, the ^{19}F signal from to the macro-looped invasion complex **C^8** (−66.90 ppm, viii in Figure 2) predominates. As with **ON^{12}**, the complex exhibits two, albeit broader and partially overlapped, signals at a higher temperature (**C^8**/**D^8**). In addition, the signal of the hairpin form **A** of the uncomplexed TAR model is increased upon heating (from 25 to 45 °C, viii−x in Figure 1). Owing to this dynamic equilibrium, a clear thermal denaturation temperature for the complex cannot be determined. However, the relative peak area of the complex suddenly starts to increase on passing 45 °C (xi−xiv in Figure 1). This phenomenon occurs prior to thermal unwinding of **A**. The relative peak areas of the ^{19}F resonance signals at various temperatures are seen in Figure 2c. It is worth noting that the composition of the structures cannot be determined reliably, since signals may be sums of overlapped coalescent and scattered signals. In spite of the potential integration errors, the profile in Figure 2c illustrates competition of intramolecular (**A⇄B**) and intermolecular (**D⇄B**) hybridization prior to thermal unwinding of **A**, and the invasion clearly takes over on passing 45 °C. In other words, at a temperature higher than 45 °C, the predominant complex is **D^8**. **ON^8**, present in excess, works as a denaturant, the efficiency of which is increased upon heating. At a temperature lower than 45 °C, the predominant complex is **C^8**, and its proportion decreases upon heating. Thermal ^{19}F profiles of the process are seen in Figure 2a(i). The UV melting profile of the mixture exhibits $T_m = 58.9$ °C, lower than that (60.7 °C) of the mixture (**A⇄B**) without **ON^8**.

Titration of **A** with **ON^8** was additionally performed in the presence of a known TAR ligand, *i.e.*, neomycin B (1.0 equiv compared to **A**, see Figure 3). Binding of neomycin itself leads to two additional broad ^{19}F signals (peaks with asterisks, vii in Figure 3), which skews integration of relative peak areas at low **ON^8** concentrations (viii in Figure 3). Upon further titration, the signal of the complex is sharpened (ix−xi in Figure 3), and a ballpark estimate of the K_d value (19.5 ± 1.7 μmol L^{-1} at 25 °C) may be determined. The site-specific binding of neomycin occurs below the bulged nucleotides of native TAR region through the minor groove.[10] It may be expected that any change in the invasion efficiency is related to this specific binding and is confined to low temperatures. Upon heating of the mixture of **A**, **ON^8**, and neomycin (1:2:1 n/n/n), the equilibrium inconsistently behaved like the mixture without neomycin, and the ^{19}F shift *vs* temperature followed the profile of **C^8** (cf. Figure 2a,c). Although the temperature-dependent behavior did not show mechanistic details, neomycin clearly enhanced the invasion. For example, in these experiments, a 1:2 mixture of **A** and **ON^8** in the presence of neomycin resulted in approximately the same conversion as obtained by the corresponding 1:8 mixture without neomycin (xi compared to v in Figure 3). The UV melting profile of the mixture gave $T_m = 62.5$ °C, which was higher than that of the mixture without neomycin (**A**:**ON^8**, 1:15 n/n).

In summary, the present study demonstrates the applicability of ^{19}F NMR spectroscopy for the characterization of RNA invasion. In addition to the obtained K_d values, temperature-dependent behavior of the complexes and their equilibrium dynamics have been monitored in a detailed manner that can hardly be achieved by any other method.

Acknowledgment. The authors gratefully acknowledge Petri Ingman for advice regarding NMR and the Academy of Finland for financial support.

Supporting Information Available: More details of the ^{19}F NMR experiments, synthesis of the oligonucleotides, thermal UV-melting profiles, ^{1}H NMR data of the **C^{12}→D^{12}** complex. This material is available free of charge via the Internet at http://pubs.acs.org.

References

(1) (a) Zamecnik, P. C.; Stephenson, M. L. *Proc. Natl. Acad. Sci. U.S.A.* **1978**, *75*, 280. (b) Stephenson, M. L.; Zamecnik, P. C. *Proc. Natl. Acad. Sci. U.S.A.* **1978**, *75*, 285. (c) Eguchi, Y.; Itih, T.; Tomizava, J. *Annu. Rev. Biochem.* **1991**, *60*, 631.
(2) (a) Židek, L.; Štefl, R.; Sklenář, V. *Curr. Opin. Struct. Biol.* **2001**, *11*, 275. (b) Fürtig, B.; Richter, C.; Wöhnert, J.; Schwalbe, H. *ChemBioChem* **2003**, *4*, 936. (c) Mayer, M.; James, T. L. *Methods Enzymol.* **2005**, *394*, 571.
(3) Latham, M. P.; Brown, D. J.; McCallum, S. A.; Pardi, A. *ChemBioChem* **2005**, *6*, 1492.
(4) (a) Kreutz, C.; Kählig, H.; Konrat, R.; Micura, R. *J. Am. Chem. Soc.* **2005**, *127*, 1158. (b) Olsen, G. L.; Edwards, T. E.; Deka, P.; Varani, G.; Sigurdsson, S. Th.; Drobny, G. P. *Nucleic Acids Res.* **2005**, *33*, 3447. (c) Hennig, M.; Munzárova, M. L.; Bermel, W.; Scott, L. G.; Sklenár, V.; Williamson, J. R. *J. Am. Chem. Soc.* **2006**, *128*, 5851. (d) Kreutz, C.; Kählig, H.; Konrat, R.; Micura, R. *Angew. Chem., Int. Ed.* **2006**, *45*, 3450. (e) Hennig, M.; Scott, L. G.; Sperling, E.; Bermel, W.; Williamson, J. R. *J. Am. Chem. Soc.* **2007**, *129*, 14911. (f) Barhate, N. B.; Barhate, R. N.; Cekan, P.; Drobny, G.; Sigurdsson, S. *Org. Lett.* **2008**, *10*, 2745. (g) Graber, D.; Moroder, H.; Micura, R. *J. Am. Chem. Soc.* **2008**, *130*, 17230.
(5) (a) Gerig, J. T. In *Biological Magnetic Resonance*; Berliner, L., Reuben, J., Eds.; Plenum Press: New York, 1978; p 139. (b) Rastinejad, F.; Evilia, C.; Lu, P. *Methods Enzymol.* **1995**, *261*, 560.
(6) Ferner, J.; Suhartono, M.; Breitun, S.; Jonker, H. R. A.; Hennig, M.; Wöhnert, J.; Göbel, M.; Schwalbe, H. *ChemBioChem* **2009**, *10*, 1490.
(7) Mei, H.-Y.; Glan, A. A.; Halim, N. S.; Mack, D. P.; Moreland, D. W.; Sanders, K. B.; Truong, H. N.; Czarnik, A. W. *Bioorg. Med. Chem. Lett.* **1995**, *5*, 2755.
(8) (a) Dalvit, C.; Ardini, E.; Flocco, M.; Fogliatto, P.; Mongelli, N.; Veronesi, M. *J. Am. Chem. Soc.* **2003**, *125*, 14620. (b) Jackson, J. C.; Hammill, J. T.; Mehl, R. A. *J. Am. Chem. Soc.* **2007**, *129*, 1160.
(9) (a) Vickers, T. A.; Baker, B. F.; Cook, P. D.; Zounes, M.; Buckheit, R. W.; Germany, J.; Ecker, D. J. *Nucleic Acids Res.* **1991**, *19*, 3359. (b) Ecker, D. J.; Vickers, T. A.; Bruice, T. W.; Freier, S. M.; Jenison, R. D.; Manoharan, M.; Zounes, M. *Science* **1992**, *257*, 958. (c) Mestre, B.; Arzumanov, A.; Singh, M.; Boulmé, F.; Litvak, S.; Gait, M. J. *Biochim. Biophys. Acta* **1999**, *1445*, 86. (d) Arzumanov, A.; Walsh, A. P.; Rajwanshi, V. K.; Kumar, R.; Wengel, J.; Gait, M. J. *Biochemistry* **2001**, *40*, 14645.
(10) (a) Wang, S.; Huber, P. W.; Cui, M.; Czarnik, A. W.; Mei, H. Y. *Biochemistry* **1998**, *37*, 5549. (b) Thomas, J. R.; Hergenrother, P. J. *Chem. Rev.* **2008**, *108*, 1172.

JA1014629